[4] C. E. Moore, Atomic Energy Levels, v. 1.
[5] D. Rosenberger, Phys. Lett. 13, 228 (1964).
[6] D. Rosenberger, Phys. Lett. 14, 32 (1965).
[7] D. M. Clunie, R. C. A. Thorn, and K. E. Treziese, Phys. Lett. 14, 28 (1965).
[8] S. E. Frish, Opticheskie spektry atomov (Optical Spectra of Atoms), M-L, 1963.
[9] D. A. Jackson, Z. Physik 75, 223 (1932).

CONTRACTION OF POSITIVE COLUMN

V. Yu. Baranov and K. N. Ul'yanov
All-union Electrotechnical Institute
Submitted 6 June 1967
ZhETF Pis'ma 6, No. 5, 622-626 (1 September 1967)

It is known that the positive column can contract at medium and high pressures. Various hypotheses were proposed to explain this phenomenon [1,2]. However, only the theory of current contraction at high pressures [3] has found experimental confirmation. The present paper is devoted to contraction of current at medium pressures ($p \sim 5 - 500$ mm Hg). The properties of the positive column were investigated in cylindrical tubes evacuated to $p < 5 \times 10^{-6}$ mm Hg and filled with spectrally pure gas (Ar and Ar + Cs). The distributions of the electron temperature T_e and density N_e over the radius were measured with double moving probes and also determined from the recombination radiation, and the distribution of the gas temperature T_a was determined by the incandescent tungsten wire method. The longitudinal electric field intensity was measured with wall probes. The electron-energy balance and the electron balance were calculated at all values of the pressure and current in six cylindrical layers.

The effective radius r_{eff} of the positive column depends on the current and on the pressure. At low argon pressure ($p < p^* \approx 5$ mm Hg) the current contracts little. At $p > p^*$ a non-contracted state exists only at currents lower than a limiting value $i < i_{lim}$, and when $i > i_{lim}$ this state becomes unstable and contraction occurs abruptly (see the figure).

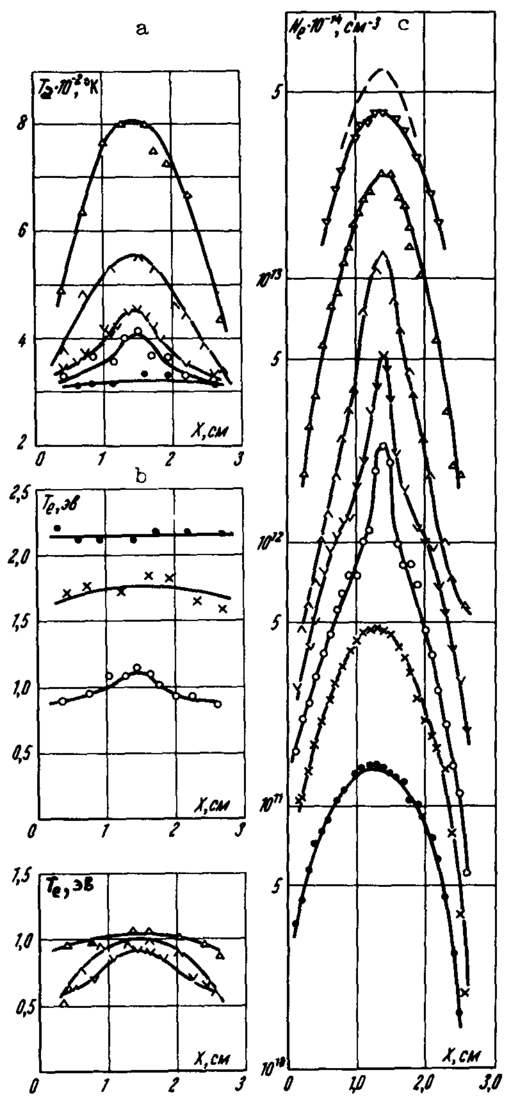

Distributions of T_a (a), T_e (b), and N_e(c) over the tube diameter (i.d. 2.6 cm) at argon pressure 20 mm Hg) in currents of 5×10^{-3} (•), 1.5×10^{-2} (×), 3×10^{-2} (o), 0.1 (v), 0.5 (^), 2 (Δ), and 5 A (∇). Dashed - density determined from absolute recombination radiation at i = 2 A.

Diffusion state at low pressures ($p < p^*$). When the current is large, the inhomogeneity of the atoms $N_a(r)$ as a result of the heating leads to only a weak inhomogeneity of $T_e(r)$, since the major role in the electron-energy balance is played by the electron heat conductivity W_T and the diffusion energy transfer W_D. For example, at p = 1 mm Hg and i = 1 A we have at the center of the discharge $W_D = 4 \times 10^6$ (erg-cm^3/sec) and $W_T = 3 \times 10^6$, while the elastic losses are $W_{el} = 6 \times 10^5$. The diffusion flux to the wall exceeded the volume recombination in the charged-particle balance at all the investigated currents (up to 5 A).

Non-contracted state at medium pressures ($p > p^*$). At medium pressures the transport processes play a lesser role in the electron-energy balance, so that inhomogeneity in $T_a(r)$ gives rise to inhomogeneity in $T_e(r)$ (see the figure). At small currents ($i < i_{lim}$), however, the mechanism whereby the charged particles are removed has likewise a diffusion character. For example, the ratio of the recombination lifetime $\tau_p = 1/\alpha N_e$ (α - effective recombination coefficient) to the diffusion lifetime $\tau_D = R^2/6D_a$ (R - tube radius, D_a - coefficient of ambipolar diffusion) for i = 15 mA and p_{Ar} = 20 mm Hg is $S = 6D_a/\alpha N_e R^2 \sim 10$. In the diffusion state, inhomogeneity of $T_e(r)$ does not lead to strong contraction.

Contracted state at medium pressures. When $i > i_{lim}$, a transition to the contracted state takes place, accompanied by sharp decreases of r_{eff} and E. With increasing current, a larger role is assumed by volume recombination (at p_{Ar} = 20 mm Hg we have $S \approx 5$ for i = 0.03 A and $S \approx 0.1$ at i = 0.5 A), and its presence contributes to the formation of a stable state. Calculation of the energy balance (see the table) has shown that the Joule heating is practically

i = 0,5 a $\quad p_{Ar}$ = 20 mm Hg

r, cm / $W \cdot 10^{-5}$ erg-cm^{-3}sec^{-1}	0,05	0,15	0,26	0,47	0,77	1,06
	110	75	50	25	10	3
	25	10	9	4	1	–

balanced by the elastic losses, and therefore T_e at each point is determined by the local discharge parameters.

With increasing current, the inhomogeneity of T_a increases and the role of diffusion decreases. Both factors intensify the contraction. With further increase in current, r_{eff} begins to increase. In argon with cesium the contraction is less pronounced, a broadening of $N_e(r)$ is observed already at small currents, and j_n (the normal current density) remains in this case constant. The power supplied is also offset by other losses in the electron-energy balance, and the elimination of the charged particles has a volume character. Thus, the contracted state is locally-collisional in a wide range of pressures ($p > p^*$) and currents ($i \gg i_{lim}$), and the energy balance has a local character. This makes it possible to construct a simple theory of current contraction. Let us consider the plane case. The system of equations is

$$N_e = N_e(T_e, N_a) \quad (1), \quad jE = W_y \quad (2), \quad W_y + K_a T_a'' = 0 \quad (3),$$

$$E = \frac{\epsilon}{l}\left[1 + \frac{2R_6}{l}\int_0^d \sigma\, dx\right]^{-1} \quad (4) \qquad p = N_a k T_a,$$

where K_a is the coefficient of atomic heat conduction, k is Boltzmann's constant, ε the source efficiency, R_b the external resistance per unit length (in the y direction), d the half-width (in the x direction), l the length of the discharge gap (in the z direction), and σ the electric conductivity. Equation (2) establishes the connection between T_e and T_e. If the electron-atom collision frequency greatly exceeds the electron-ion collision frequency, $\nu_{ea} >> \nu_{ei}$, then the characteristic scales of T_a and T_e are of the same order, and the scale of N_e is smaller than the scale of T_e by a factor $U_e = E_i/kT_e$, owing to the presence of the exponential factor in (1). It is this which causes the contraction in the case of strong temperature inhomogeneity. When $\nu_{ea} << \nu_{ei}$, the density N_a, whose inhomogeneity gave rise to the contraction, no longer enters in (2), and the scales of T_e and N_e are of the same order and greatly exceeds the scales of T_a and N_a. Where $\nu_{ei} \sim \nu_{ea}$, the distributions $N_e(x)$ and $T_e(x)$ become more homogeneous, giving rise to an increase in r_{eff} and to existence of J_n. These regularities can be traced by means of a simple example. Local equilibrium with $T = T_e$ frequently exists in metal vapor. It is then possible to use in lieu of (1) the Saha equation. Let us consider for concreteness an Ar + Cs mixture at a low degree of Cs ionization. The elastic electron losses are determined by scattering from Ar, the cross section being $\sigma_{ea}^{4} \sim T_e$. Let $n_e = N_e/N_e(0)$, $t_e = T_e/T_e(0)$, $t = T_a/T_a(0)$ and $\varepsilon = \nu_{ei}(0)/\nu_{ea}(0)$. For $\varepsilon << 1$ and $T_e(0) >> T_a(0)$ we have

$$n_e = 1 - \mathrm{th}^2\left(\frac{x}{2a}\right), \quad t_e = \left[1 - \frac{2kT_e(0)}{E_i}\ln\left(1 - \mathrm{th}^2\frac{x}{2a}\right)\right]^{-1}, \quad t \sim t_e^2 \,,$$

$$i = \sigma(0)E\cdot 4a\left[1 - 2/(e^{d/a} + 1)\right], \quad a^2 = 2K_a T_a(0)/W_y(0)\,U_e(0)\,,$$

where a is the characteristic dimension of the thermal conductivity. The quantity 0.5a can be taken to be the contraction radius. a decreases with increasing current and pressure. When $a << d$ strong contraction takes place. When $\varepsilon >> 1$ we get $t_e \approx n_e$ and the contraction is weaker. As the current increases, r_{eff} first decreases, and then, when $\varepsilon \sim 1$ in the center, it increases. Assuming that $\nu_{ei} \sim \nu_{ea}$, we have

$$i_n = e\,\bar{v}_e N_a \left(\frac{m_e}{m_a}\right)^{1/2} \frac{\bar{\sigma}_{ea}}{\bar{\sigma}_{ei}}\,,$$

where $\bar{v}_e$ is the thermal velocity of the electrons, $\bar{\sigma}_{ea}$ and $\bar{\sigma}_{ei}$ the electron-atom and electron-ion collision cross sections, and m_e and m_a the electron and atom masses. The current density j_n calculated from this formula coincides with that measured in Ar + Cs.

Deviation from equilibrium with $T = T_e$, due to emergence of the radiation and to violation of the equilibrium electron velocity distribution in the volume state, leads to intensification of the contraction. First, the non-equilibrium system requires larger values of T_e and E at the same value of the current. This increases the power W_E released in the discharge and the inhomogeneity of $T_a(r)$. Second, a change in $T_e(r)$ leads to a much stronger change in $N_e(r)$ than in the equilibrium case. This apparently causes the very strong contraction of the current in pure argon. The transition of the current to the contracted state is connected with the fact that the diffusion mechanism of eliminating the charged particles gives way to the volume mechanism. The recombination rate is usually proportional to N_eN_i, and therefore the transition to the contracted state occurs first on the discharge axis, and a diffuse 'halo' remains on the periphery (see the figure), with a characteristic dimension that decreases with increasing current.

[1] K. Kenty, Phys. Rev. 126, No. 4, (1962).
[2] Yu. B. Golubovskii, Yu. M. Kagan, and V. I. Lyagushenko, Opt. i spektr. 20, 561 (1966) and 21, 525 (1966).
[3] W. Elenbaas, High Pressure Mercury Vapor Discharges, 1950.

LOSS MECHANISM IN PRIMARY OPTICAL BREAKDOWN

V. E. Mitsuk and V. A. Cherikov
Physics Department, Moscow State University
Submitted 14 June 1967
ZhETF Pis'ma 6, No. 5, 627-631 (1 September 1967)

Primary optical breakdown of a gas in the focus of a laser at pressures on the order of atmospheric can be satisfactorily explained on the basis of the electron-avalanche mechanism proposed by Ya. B. Zel'dovich and Yu. P. Raizer [1]. Within the framework of the avalanche theory it is also possible to account for processes that influence the development of the electron avalanche, such as photoionization of excited atoms [2] and diffusion losses [3]. In a number of cases the development of the avalanche may be greatly influenced also by impacts of the second kind between electrons and excited atoms, since these accelerate the avalanche. The time constant θ of avalanche development is given by

$$\theta^{-1} = \frac{\alpha}{\theta_0} - \frac{1}{\tau_D}, \qquad (1)$$

where $\theta_0^{-1} = \dot{\varepsilon}/I_1$

$$\dot{\epsilon} = \dot{\epsilon}_0 - \dot{\epsilon}_1 = \frac{e^2 E^2 \nu_e}{m(\omega^2 + \nu_e^2)} - \frac{2m}{M}\epsilon \nu_e$$

is the rate of growth of the energy ε of the electron as a result of deceleration absorption of light quanta ħω in collisions between the electrons and the neutral atoms, I_1 is the effective ionization threshold, and α is the probability that the electron jumping through an excitation-loss band of width $\Delta = I_1 - \varepsilon^*$ (ε^* is the energy of the first excited level). The procedure for accounting for the photoionization of the upper levels, proposed in [2], leads to the substitution $\alpha' = \alpha + \beta(1 - \alpha)$, where β is the probability calculated by means of formula (7.2) of [1]. To take impacts of the second kind into account, we introduce the parameter $\gamma = W_{II}/W_I$ into account, characterizing the ratio of the probabilities of impacts of the second and first kinds. As a result of a collision of the second kind with an excited atom, the electron acquires an energy that is either sufficient for subsequent ionization of the